Version of Record: https://www.sciencedirect.com/science/article/pii/S0260877421003265
Manuscript_0fd1294cd7646ed3b2fc7f1893e5cc71

Reconstitution of fruit powders: a process – structure – function approach

Naïma GAUDEL[a], Claire GAIANI[a], Yogesh M. HARSHE[b], Jana KAMMERHOFER[b], Matthieu POUZOT[b], Stephane DESOBRY[a], Jennifer BURGAIN[a*]

[a]Université de Lorraine, LIBio, F-54000 Nancy, France

[b]Nestlé Research, P.O. Box 44, CH-1000 Lausanne 26, Switzerland

*Corresponding author: jennifer.burgain@univ-lorraine.fr

Graphical Abstract

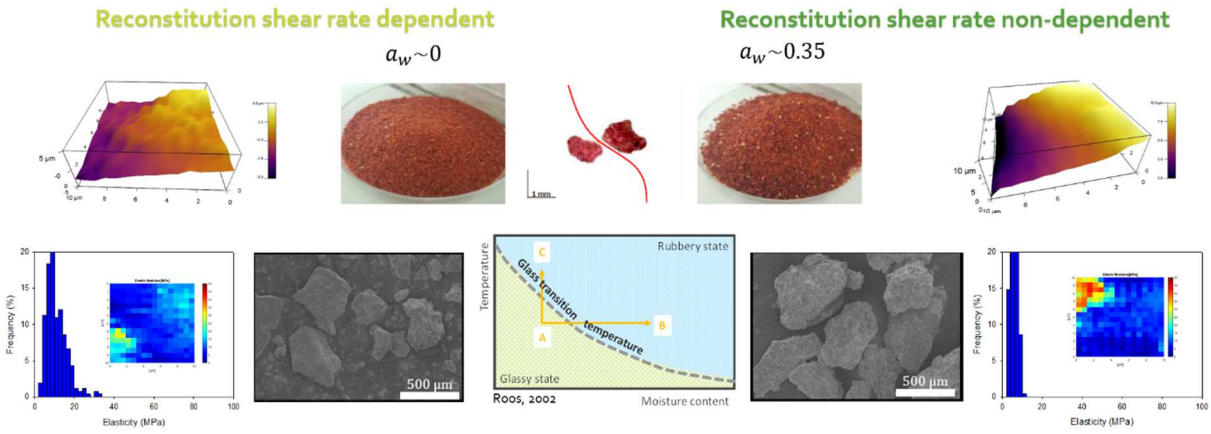

Schematic explanation of the relationship between water activity and fruit powders behavior during reconstitution.

Abstract

Reconstitution of six fruit powders, compacted and non-compacted, were studied. It appears that powder reconstitution behavior under sheared conditions was significantly different with regards to the water activity (a_w). At low a_w, the powders exhibit a glassy state with a stiff surface measured by Atomic Force Microscopy and porous/angular shapes were observed by

Scanning Electron Microscopy. In that case, increasing the shear rate accelerated the kinetics of reconstitution by improving water penetration through particle surface pores thus reducing the reconstitution time. Therefore, the reconstitution is shear rate dependent. At high a_w, the powders are under a rubbery state with a soft surface and a smooth shape. Under these environmental conditions (i.e. above powder's glass transition temperature), increasing the shear rate did not improve their reconstitution. Therefore, the reconstitution kinetics is not shear-dependent in the stirring rate studied (from 800 to 1500 rpm). It is suggested that the viscous layer created on the particle surface blocks the entrance of water for these powders rich in sugar and presenting low glass transition temperatures.

Key words

Fruit powder; reconstitution; shear rate; glass transition temperature; compaction; water activity

1 Introduction

Fresh fruits are usually dried as they contain about 90 % water by weight and reducing the water activity in the product allows for food preservation (*i.e.* reducing microbial and enzymatic activities). Indeed, browning and loss of nutritional value are typical of fresh fruits even at ambient temperature and relative humidity. In the powder form, the stability and the functionality of the ingredients composing fruits are maintained (Fitzpatrick and Ahrné, 2005). However, fruit powders contain a high quantity of low molar mass sugars with low glass transition temperature (T_g) (Fang and Bhandari, 2011). The direct consequence is that fruit powders are highly hygroscopic and sticky at high temperatures but also at ambient temperature if the water content is not well mastered. This feature causes the powder

adhesion to surfaces and powder caking during the storage, which affects the quality of the final product (Gabas et al., 2007; Fabra et al., 2011). The T_g is one of the most important parameters to take into account during powder storage. Indeed, the phenomenon of glass transition is the gradual and reversible transition of amorphous materials from a hard and "glassy" state into a viscous and rubbery state as the temperature and/or the moisture content is increased. The glass transition is also linked to the water activity and water as a strong plasticizer decreases the T_g. Also, the glass transition temperature depends on the molecular mass as the T_g of monosaccharides, disaccharides, oligosaccharides and polysaccharides increases with increasing their molecular mass (Roos, 2002). If the glass transition is reached during powder storage, unexpected phenomena can happen that affect powder functionality such as reconstitution ability. One way of influencing this powder functionality is the granulation process.

Granulation is a particle size-enlargement process carried out to improve flowability, compaction and homogeneity of powders. This is an important process in many industries including the food, pharmaceuticals and chemical industries. Roller compaction is a process used for dry granulation typically employed in the food industry to increase the flowability of a powder by forming granules of large size and density (Kleinebudde, 2004). During this processing step, a powder blend passes through two counter-rotating rolls that compact the blend into ribbons. The ribbons subsequently are milled into granules of a desired size distribution. This granulation process induces structural and physical changes by increasing the size of the particles and the voids between particles, but also by playing on powder bulk properties, especially by decreasing the bulk density (Rajniak et al., 2007). As a consequence, the wetting step is improved by the production of particles with large pores, which facilitate the entrance of water into particles (Hogekamp and Schubert, 2003). Dispersibility is also

related to the increased particle size (Goalard et al., 2006). Thus, granulation will impact the reconstitution ability.

Reconstitution of powdered ingredients is of particular importance to both manufacturers and consumers as a target of consumption quality (Fang et al., 2011). Reconstitution is highly dependent of both operating conditions and material properties. The objective is to restore the fresh product functional properties, especially for heat-sensitive food products such as vegetables and fruits powders (Lopez-Quiroga et al., 2019). Reconstitution of food powder generally consists of four steps or phases: wetting of powder particles, sinking, dispersing, and particles completely dissolving in solution (Forny et al., 2011; Mitchell et al., 2015). Wetting is the first step where the particles contact liquid, the physicochemical properties of particle surface is of major importance for improving initial step. Dispersing and dissolution are the critical phases where primary particles start to release materials from the particle surface into the liquid. Once any of these steps is limited, the time for the whole reconstitution is prolonged. Particularly, in the case of fruit powders, the dissolution cannot be fully achieved due to the presence of many insoluble polysaccharides. Additionally, different steps can overlap that makes understanding the global rehydration process more complicated (Schubert, 1993).

The influence of reconstitution conditions (stirrer speed, mixing systems, temperature, and viscosity) is also known to influence the reconstitution time. For dairy powders, authors (Jeantet et al., 2010; Andre et al., 2012) show that increasing temperature and/or agitation resulted systematically in decreasing the reconstitution time. Also, their respective influences were compared and increasing the temperature by 4 °C was found to have the same

87 influence on reconstitution time than multiplying by two the stirring speed. On the best
88 knowledge of the authors, this type of study crossing the impact of the process parameters
89 were never done on fruit powders. Because of various origins, particle size and shape
90 distributions, chemical composition, surface composition, and physical properties,
91 reconstitution is highly variable. Again, many data were acquired for dairy powders (Gaiani et
92 al., 2006, 2007a, 2007b, 2009), hydrocolloids (Wangler and Kohlus, 2018), biopolymers
93 (Wangler et al., 2019), but not yet for fruit powders.

94 With regard to process, powder composition and structure complexity, knowledge of fruit
95 powder reconstitution is clearly insufficient in comparison with other food powders (*i.e.* dairy
96 powders). Therefore, the objectives of this study were to investigate the impact of structure
97 (compacted or non-compacted), composition (various fruits), stirring speed and material state
98 (glassy vs rubbery depending on the a_w) on fruit powder reconstitution.

99

100 # 2 Material and methods

101 ## *2.1 Fruit powders*

102 Six industrial fruit powders of different nature were analyzed (**Figure 1**):

103 - Fruit-based powders non-compacted and compacted, denoted FNC and FC,
104 respectively.
105 - Red mix powders non-compacted and compacted, denoted RNC and RC, respectively.
106 - Purple mix powders non-compacted and compacted, denoted PNC and PC,
107 respectively.

108 Each formulation contains different mixes of fruit powders. To obtain compacted powders,
109 each mix of non-compacted powders had undergone a compaction process to form larger

particles. Therefore, for one similar chemical composition, two powders were studied: non-compacted (NC) and compacted (C).

2.2 Storage conditions

All the powders were stored at two conditions that are $a_w \sim 0$ and $a_w \sim 0.35$ before using them for experiments. In order to maintain a low water activity (*i.e.* $a_w \sim 0$) and prevent powder caking, powders were stored at 20 °C in a desiccator (Nalgene cabinets) containing phosphorus pentoxide (P_2O_5 from Sigma Aldrich) as drying agent. For the second condition, powders were stored at 20 °C in another desiccator containing magnesium chloride salts ($MgCl_2$ from Sigma Aldrich) to maintain an $a_w \sim 0.35$, in order to mimic ambient conditions. The value of water activity was often verified and determined using a Hygropalm HP23-AW (Omni Instruments, UK) before using the powders for experiments. This device, calibrated using salts whose water activity is known, has a measuring range equals 0 to 1 with an accuracy of ± 0.008, over a temperature range comprised between −10 °C and 60 °C. A sample of powder (typically around 15 g) was poured into a polypropylene container, and the water activity measurements were realized using an electrolytic sensor. Three repetitions were performed for each sample.

2.3 Surface properties

2.3.1 Optical imaging

The influence of water activity on visual properties was evaluated with classical imaging. Pictures of the fruit powders studied were taken with a classic camera. Pictures with an optic microscope (Dinolite, 5 Megapixel Edge sensor, 10 – 200× magnification, polarizer and flexible LED control) were also recorded.

134 2.3.2 Scanning Electron Microscopy

135 A high-resolution field-emission scanning electron microscope (SEM) type JEOL JSM-7100F
136 supplied with a hot (Schottky) electrongun (JEOL Ltd., Tokyo, Japan) and having a resolution
137 around 1 nm at 30 kV was used to investigate the surface morphology and topography of fruit
138 powders at two different water activity values. The equipment was operated at 1 kV. Samples
139 were mounted onto SEM stubs by fixing them on a carbon double-sided adhesive tape.
140 Finally, a coating of iridium was applied to the samples until reaching around 10 nm coating
141 thickness.

142 2.3.3 Atomic force microscopy (AFM)

143 Prior to AFM experiments, fruit powders were glued onto the surface of circular glass. The
144 surface topography of fruit powder particles was probed in air with a MFP3D-BIO instrument
145 (Asylum Research Technology, Oxford Instrument, Manheim, Germany) using gold coated
146 AFM-tips (NPG, Bruker SAS, Palaiseau France). The used scan area was 10 µm×10 µm
147 (corresponding to 512 lines). Mechanical properties of individual particles were probed at the
148 nanoscale by AFM nanoindentation technique. Measurements were performed in air and at
149 room temperature with stiff cantilevers (MPP-13100 with 200 N/m spring constant). The
150 cantilever was calibrated onto sapphire substrate. The force-distance curves recorded by AFM
151 were analyzed according to the theoretical Sneddon model to extract the mechanical
152 properties (*e.g.* elasticity).

153

154 2.3.4 X-ray photoelectron spectroscopy

155 The elemental surface composition of FNC and FC (up to 10 nm depth) was measured by X-
156 ray Photoelectron Spectroscopy (XPS) (Gaiani, 2006; Rouxhet et al., 2008). Before analysis,

157 the samples were outgassed under vacuum for 24 h. Spectra were obtained using a KRATOS
158 Axis Ultra X-ray photoelectron spectrometer (Kratos Analytical, Manchester, UK) equipped
159 with a mono-chromatic Al Kα X-ray ($h\nu$ =1 486.6 eV) operated at 150 W. The analysis area
160 equaled 700 µm × 300 µm and spectra were collected at normal take-off angle 90°. Four
161 repetitions were performed for each sample.

162 ### *2.4 Physical and chemical properties*

163 #### 2.4.1 Differential scanning calorimetry

164 Differential scanning calorimetry (DSC 2500, Discovery DSC Series, TA Instruments)
165 measurements were used to investigate the glass transition in fruit powders. Samples of
166 powder, pre-weighed (around 10 mg), were sealed in Tzero aluminum hermetic pans with a
167 mechanical crimp. These pans were placed in parallel to an empty capsule, which was the
168 reference. The samples were under protective nitrogen and the procedure was fixed to
169 perform a first round of heating from -20 °C to 50 °C at 10 °C.min^{-1} rate, followed by a cooling
170 from 50 °C to -20 °C at the same rate. A second heating from -20 °C to 50 °C at 10 °C.min^{-1}
171 rate was then performed, and the glass transition temperature ($\mathrm{T_g}$) extracted from this
172 heating were studied. Two repetitions at least were performed for each sample.

173 #### 2.4.2 Particle size distribution

174 The particle size distribution was obtained using a laser diffraction granulometer (Mastersizer
175 3000, Malvern Instruments, UK) equipped with Aero S dry powder dispersion unit. All samples
176 were dispersed at 1 bar air pressure. The feed rate and the hopper length values were
177 adjusted to obtain a correct obscuration between 1 and 15 %. The particle size distribution
178 was calculated from Mie theory, and provided as a volume density function. The particle size
179 estimator was the d_{50}, which means that 50 % of particles have a lower diameter. The span
180 value was used as a polydispersity indicator, and is given by:

Equation 1 $$span = \frac{d_{90} - d_{10}}{d_{50}}$$

where 10 %, 50 % and 90 % of the sample particles are smaller than the diameter d_{10}, d_{50} and d_{90},respectively. Three repetitions were performed for each sample.

2.5 Reconstitution properties

2.5.1 Conductivity measurements during reconstitution

The time evolution of the conductivity was obtained using a portable conductivity S7 - Standard Kit with a sensor (INLAB 738 ISM from Mettler Toledo Seven2Go). The calibration of the sensor was made at T = 25 °C with a calibration liquid at a conductivity 1 413 µS.cm^{-1}. The time duration of the measurement was adapted depending on the sample. Conductivity measurements were realized in a beaker of 200 mL that was put in water bath with circulating water supply in order to have a constant and fixed temperature (25 °C). A volume of 100 mL of water was poured into the beaker and the powders were reconstituted under specific TS conditions (10 ± 0.1 g). The powders were blended into water, thanks to a bar magnet of length 3 cm, with a magnetic stirrer in a range of stirring speed values (from 800 to 1 500 rpm). Three repetitions were performed for each sample.

2.5.2 Particle size distribution during reconstitution

The particle size during reconstitution was followed using the laser diffraction granulometer (Mastersizer 3000, Malvern Instruments, UK) equipped with the Hydro MV unit. The particles were dispersed in 120 mL dispersant volume with a stirrer (0 – 3 500 $\pm$ 10 rpm). The dispersant used was distilled water. The samples passed through a measuring cell using a centrifugal pump (flow rate Q = 0 – 2 L.min^{-1}). The particle size was probed with a sequential combination of measurements with red and blue light sources. Experiments were conducted with powders stored at $a_w \sim 0$ and $a_w \sim 0.35$. The stirring speed was fixed at 2 000 rpm, and

water temperature at T = 24 $\pm$ 2 °C. For one measurement, the integration time of each light source was adapted depending on the sample and its kinetics (typically between 1 and 5 sec) in order to have reliable and repeatable results. The time variation of particle size distributions was assessed choosing the number of measurements and the delay between each one, depending on the sample. The mass of the studied samples, typically between 0.02 and 0.30 mg, were adapted to obtain obscuration between 1 and 30 % depending on the particle size. For instance, the mass of powder rehydrated into the device was chosen at m = 0.15 g and m = 0.30 g for FNC and FC, respectively. Two repetitions were performed for each sample.

3 Results and discussion

3.1 Particle size, shape and visual aspects

The particle size distributions of the six fruit powders (three fruit compositions and two structures per composition) were measured at two water activity values (**Figure 2**). Information related to these functions such as the mean diameter d_{50}, the $\mathbf{span}$ value and the percentage increase of d_{50} between two a_w values are presented in **Table 1**. Visual/optic microscopy and electronic microscopy images are presented in **Figures 3** and **4**, respectively.

Impact of compaction. The compaction process leads systematically to a high mean diameter, and also produces only monodisperse population of particles even if the non-compacted powder has bimodal distribution (for instance, FNC/FNC and RNC/RC powders). From images, non-compacted powders seem to have a particle size around a hundred microns, which was confirmed by the determination of the d_{50}. Also, compaction process seems to produce more

homogeneous size distribution (images), which is confirmed by a smaller span value. Finally, images suggest that compaction process led to angular shapes particles with high rugosity.

Impact of water activity. From size measurements, increasing the water activity value leads to an increase of the mean diameter, and a decrease in span value. This can be explained by the apparition of two populations: the lowest size population represents the increase in mean diameter with increasing a_w, while the higher size population (around $d{\sim}1\ 000$ µm) is due to the agglomeration of individual particles. An increase in moisture content leading to an increase in free volume due to the formation of hydrogen bonds may also impact the particle size (Jadhav et al., 2009; Moghbeli et al., 2019). The non-compacted powders are much more sensitive to the impact of water activity regarding their mean diameter, in comparison with the compacted ones as shown by the percentage increase of d_{50}. Moreover, for compacted powders, the greater the diameter at $a_w{\sim}0$, the less it increases with increasing a_w. Images suggest a smoother surface at $a_w{\sim}0.35$, in comparison with the angular shape observed at $a_w{\sim}0$. This suggests a sticky surface that may explain the agglomerates for non-compacted powders, and a change in powder surface. Increasing water activity value seems to change the powder surface and the particle size (Liu et al., 2010). Although it is not visible using SEM imaging due to the coating, this could also change the porosity at the surface of the particles, and thus influencing the reconstitution properties (entrance of water into the structure). Finally, optical images also show a clear difference in color when increasing the water activity value, in agreement with Jiang et al. (Jiang et al., 2013). These pictures suggest a change in surface properties between $a_w{\sim}0$ and $a_w{\sim}0.35$, that may impact later the reconstitution by clogging pores where water could penetrate. This aspect will be discussed later in the results and discussion part.

3.2 Powder surface characterization

Impact of compaction. XPS analysis was performed on FNC and FC in order to evaluate the impact of the compaction process on the surface composition for powders having similar bulk composition. Three common chemical elements were detected at the surface of the powders: carbon C, oxygen O, nitrogen N with mineral traces (K and P). The detection of nitrogen suggests the presence of proteins at the surface. For FNC powder, minor elements were detected in very low concentration: potassium K and phosphorus P (Figure 5a). Regarding the results of the surface atomic concentration of chemical elements, there is no impact of the compaction process on the surface composition of the studied powders. Moreover, the analysis of carbon bonds (Figure 5b) reveals again no significant influence of the compaction process on the carbon element. Almost the same atomic concentration of C-C bonds and C-O bonds (50 % - 50 %) is observed. This suggests that fruit powder surfaces are mainly composed of polysaccharides. Ratios between carbon element and oxygen element, and C-C bonds and other C bonds (C-O, C=O, O-C=O) were calculated (Figure 5c). These ratios give information about the hydrophilic/ hydrophobic nature of the powder surface. It appears that the surface is mostly similar and that the compaction had no impact measured by XPS. The XPS results suggested that potential differences in reconstitution properties should not come from a chemical point of view in term of surface composition (Nijdam and Langrish, 2006; Murrieta-Pazos et al., 2012).

Impact of water activity. To go further and quantify the impact of water activity on the surface of fruit powders, surface topography and nanomechanics were performed by AFM (Figure 6). Regarding the measurements at $a_w \sim 0.35$, it was very difficult to keep the contact between the AFM tip and the surface, probably due to a thin layer of water present at the surface as already reported in literature (Eaton and West, 2010). For nanoindentation, it can be seen

that the distribution is centered at 10 MPa for the powders stored at $a_w \sim 0$ and a shift to lower values (5 MPa) was observed for the powders stored at $a_w \sim 0.35$. This means that powders stored at higher water activity present a softer surface compared to the ones stored at $a_w \sim 0$. The elasticity maps reveal that some regions are stiffer than the rest of the surface meaning that nanomechanical properties are inhomogeneous at the particle surface. It appears that increasing water activity impacts the surface properties of powders. DSC measurements were obtained for the six fruit powders studied at two a_w, in order to determine the influence of water activity on the glass transition temperature evolution (Table 2). For all powders, a glass transition clearly appeared and the endpoint glass transition temperature (T_g) was extracted. From a general point of view, glass transition occurred at lower temperature for non-compacted powders than for compacted ones. This result may be due to both an increase in surrounding pressure and a decrease in water content as already reported in literature (Jadhav et al., 2009; Lopez-Quiroga et al., 2019; Moghbeli et al., 2019). Furthermore, a significant decrease of the glass transition temperature T_g was observed with increasing water activity value, which could be explained by an increase in free volume (Roos, 2002). The most important result is that all powders (whatever the compaction and the relative activity) are above or slightly below their glass transition at ambient temperature (T=20 °C). At a_w=0, some samples are in the glassy state (FC, PNC and PC powders) and some (FNC, RNC, RC powders) are just above Tg, leading to a transition from a glassy state to a rubbery state. As these samples are close to the transition from glassy to rubbery state, in these conditions, at microscopic scale the matrix is partly at rubbery and partly at glassy state. At a_w=0.35, all samples are at the rubbery state. Also, for material containing sugars, like fruit powders, this transition from brittle solids to sticky materials is responsible for caking and particle size increase as previously observed by visual and microscopy images.

297 Therefore, powders at $a_w \sim 0.35$ are under a rubbery state whereas the one maintained at
298 low a_w are partly under a glassy state. As seen in **Figures 3** and **4** and already discussed,
299 particle surface is rougher and more angular at $a_w \sim 0$. It confirms that a material transition
300 occurred; this transition being correlated to a modification of the nanomechanical properties
301 at the particle surface. These surface changes should influence the reconstitution, particularly
302 concerning the initial interaction between particle and water, during the wetting and swelling
303 steps.
304
305 ### *3.3 Powders reconstitution ability*
306 ***Conductivity measurements.*** The conductivity values were followed with time during
307 reconstitution of the six studied powders at a water activity ~ 0 and ~ 0.35 (**Figure 7**). An
308 example of the typical time evolution of the conductivity and the extraction of the
309 reconstitution time (τ_R) are plotted in **Supplementary material 1**. The conductivity value
310 quickly increases and then reaches a constant value. The reconstitution time was then
311 evaluated by considering that the reconstitution is reached when the conductivity value
312 equals 90 % of the maximum conductivity value (Mitchell et al., 2015, 2019).
313 The non-compacted powders have systematically faster reconstitution than the compacted
314 ones, thus resulting in shorter reconstitution times. This is mainly due to the particle size,
315 which is higher for the compacted powder and add a step of disintegration of the granules.
316 However, two distinct behaviors appear concerning the evolution of τ_R with shear, which
317 seems to depend on the water activity value. At low water activity, the evolution of τ_R with
318 the stirring speed, obtained by conductivity measurements, exhibits that an increase in
319 stirring speed leads to a decrease of τ_R. This comes from a better water entrance through
320 particle surface porosity and therefore a faster reconstitution of particles under applied

shear. This result is usually observed by authors for food powders and more particularly for dairy powders (Andre et al., 2012). But at a higher water activity (~ 0.35), the behavior during reconstitution is significantly and systematically changed. Although reconstitution times are higher for compacted powders than for non-compacted, τ_R does not evolve significantly with shear for a given fruit powder, in the range of stirring speed studied (800 – 1 500 rpm). Therefore, it is observed that the reconstitution of these six powders is shear dependent at low relative humidity and non-shear dependent at a higher relative humidity. This result was totally unexpected and to the best of our knowledge, it was never observed until now. This could come from the fact that powder surface at $a_w \sim 0.35$ is partially hydrated leading to a swelling of the particles that is reflected by the particle size increase. In that case, the limiting factor for powder reconstitution is mainly the diffusion of water inside the structure. This could also explain the observation that for some powders (FNC, RC, PNC and PC) and at low stirring speed value (N = 750 - 800 rpm), τ_R at $a_w \sim 0$ is lower than τ_R at $a_w \sim 0.35$. These results clearly put in evidence that increasing water activity value leads to a non-dependence of shear on the reconstitution time, in the range of stirring speed studied.

Particle size distribution (PSD). The experiments of reconstitution by particle sizing were performed for FNC and FC powders in order to confirm the results obtained by conductivity measurements and verify the final state of the powders. The results of the time evolution of the volume density functions are presented in the form of a map with both the initial and the final PSD at $a_w \sim 0$ and $a_w \sim 0.35$ for FNC and FC (**Figure 8**). Although a larger particle size at the beginning when increasing the water activity, a given composition powder leads to an identical final volume density function, irrespective of the initial particle structure (compacted or non-compacted) and the water activity value. Rather, these two parameters (structure and a_w) influence the reconstitution time. It can also be noticed that the initial and final volume

density functions of FNC at $a_w \sim 0$ are almost the same, with a slight increase of the volume density for the main peak ($d \sim 200$ µm) and a slight decrease of the secondary peak ($d \sim 30$ µm). This result suggests that mainly dispersion step occurs during reconstitution of this powder. Indeed, disintegration of small agglomerates into primary particles (from the main peak) and small particles (from secondary peak) would explain the observations. The time evolution of the mean diameter d_{50} extracted from volume density functions is plotted in Figure 9. The data are well fitted to an incomplete dissolution model derived from the Noyes-Whitney model (Cogswell et al., 2006). This model was proposed and successfully used by Fang *et al.* (Fang et al., 2011) in the case of the reconstitution of milk protein concentrate by measuring the particle size through optical images. The model is defined as:

Equation 2
$$d_{50}(t) = (d_0 - d_\infty) \exp\left(-\frac{t}{\tau_{PSD}}\right) + d_\infty$$

where d_0 is the initial mean diameter (dry case), d_∞ is the final mean diameter (at the end of the rehydration) and τ_{PSD} is the characteristic reconstitution time of the particle size distribution. The characteristic reconstitution time and the final mean diameter value extracted are presented in Table 3. As already observed with the conductivity measurements, the compaction process increases the reconstitution time because a step of granule destruction adds up compared to non-compacted powders. The results also show that increasing the water activity value leads to an increase in reconstitution time. The results from granulometry during reconstitution provide a new piece of information: the final mean diameter depends neither on the water activity value nor the compaction process. This means that powders reach the same final state after total reconstitution.

3.4 Relationships between powder process, structure and function at two water activities

The relationships between process (compaction), structure (glassy/rubbery state) and function (reconstitution ability) is established with this multi-scale approach. From a macroscopic point of view, fruit powders are particularly sensitive to their storage environment (Islam et al., 2016). The observations demonstrate a transition from a glassy state to a rubbery state, easily visible by a color and aspect changes (caking due to the plasticizing effects of water on the particle surface) with the water activity increase at typical storage temperature *(i.e.* around 20 °C). The glass transition can appear either by increasing the temperature and/or the water activity (Roos, 2002). Here, a clear impact of water activity on macroscopic fruit powders characteristics was observed. It was already shown an inverse relationship between T_g and water activity for fruit powders (Tonon et al., 2009; Goula and Adamopoulos, 2010; Islam et al., 2016). From a microscopic point of view, this transition from angular particles to smoother ones with a large increase in the mean diameter (swelling of particles) was observed with increasing water activity. These microscopic modifications are observed by both SEM and PSD with the calculation of the d_{50} increase with relative humidity. Again, similar observations were previously made for sugar rich powders (Tonon et al., 2009; Goula and Adamopoulos, 2010; Islam et al., 2016). Finally, a transition from a stiff and brittle surface to a soft surface using nanomechanics was observed with increasing water activity value. The evolution of the Young's modulus is in agreement with both macroscopic and microscopic evolution of the powders.

It is well admitted that many factors can affect the powder reconstitution. It may be the method of reconstitution (type of stirrer, configuration, intensity of agitation, water temperature ...) (Fitzpatrick et al., 2000; Jeantet et al., 2010) or the material properties (particle size distribution, density, porosity, morphology, surface

390 hydrophilicity/hydrophobicity...) (Gaiani et al., 2007a; Murrieta-Pazos et al., 2012). The
391 novelty in this study is that it has been shown that shear rate does not affect the
392 reconstitution behavior at high water activity value (~ 0.35) whereas it impacts at low water
393 activity value (~ 0). This non-dependence to shear was never observed for food powders and
394 more particularly dairy powders largely studied at various shear rates (Richard et al., 2013).
395 Nevertheless, the composition dairy powders is very different than fruit powders.
396 Furthermore, the glass transition temperature of fruit powders is lower compared to milk-
397 based powders due to high fraction of sugars. Recently, a study of Wangler *et al.* (Wangler et
398 al., 2019) on the reconstitution of biopolymer powders with different coating demonstrated
399 the importance of a viscous layer on the dissolution/non-dissolution rate. The authors
400 showed that a biopolymer particle exhibiting a layer with low viscous cohesion reconstitutes
401 first by capillarity and then by diffusion. On the contrary, increasing the layer thickness due to
402 swelling leads to an entrance of the water mainly by diffusion. Regarding our results on fruit
403 powders, an analogy can be made with reconstitution of fruit powders depending on the
404 water activity. Indeed, mainly three reconstitution steps are relevant to our study: the
405 wetting, the swelling and the dispersion/dissolution. The dispersion/dissolution rate mainly
406 depends on the specific surface area in contact with water, which is higher for non-
407 compacted powders. Thus, the effect of compaction process is very important at this
408 reconstitution step. At $a_w \sim 0$, powders are under a glassy state and their porous surface help
409 both surface erosion and the entrance of water by capillarity, following by water diffusion. In
410 this case, increasing shear leads to a decrease of the reconstitution time. However, for
411 particles under a rubbery state (at $a_w \sim 0.35$), the wetting/swelling steps have already begun,
412 resulting in the collapse of the pore network, making appear a viscous layer. In this case,
413 increasing shear does not improve water entrance due to the viscous layer on the surface of

414 the particles. Thus, for this elevated relative humidity, diffusion may be the limiting step, *i.e.*
415 the step with which we can improve the reconstitution. In this particular case, to promote the
416 rate of reconstitution speed it may be useful to increase the temperature to reduce the
417 viscosity in the viscous layer rather than increasing the shear rate. The hypothesis proposed in
418 this work is presented in a schematic in Figure 10.
419
420 ## 4 Conclusion
421 In the present work, the reconstitution of fruit powders was evaluated. Three mixes were
422 used in a non-compacted and a compacted state. First of all, it was found that the compaction
423 process only delays the entire reconstitution process but the final state was identical for each
424 mix, irrespective of the initial structure of the powder. Secondly, the crucial role of water
425 activity was evidenced and its impact on the kinetics of powder reconstitution was evaluated.
426 In fact, at low water activity, a shear-dependence of reconstitution kinetics was observed
427 indicating that the increase in the stirring speed improved the entrance of water inside a
428 particle. In that case, powders were under the glass transition temperature, so they were in
429 the glassy state. This was evidenced by both DSC measurements and also by imaging (SEM
430 and AFM), which reveals porous/angular shapes and stiff particles. On the contrary, at a
431 higher water activity (~ 0.35), the powders were above the T_g due to the plasticizing effect of
432 water. The powders were in the rubbery state and the particles appeared smooth and soft.
433 Under these circumstances, the kinetics of reconstitution was found independent of the
434 stirring speed. This behavior may have resulted from the formation of a viscous layer at the
435 particle surface, which is responsible for the closure of the porosity at the particle surface.
436 The main consequence is that the entrance of water into the internal structure is significantly

reduced. Thus, diffusion becomes the rate controlling step for powder reconstitution. Hence, increasing shear rate which would typically enhance the mass transfer coefficient on the surface is not observed under these circumstances.

Acknowledgements

The authors acknowledge support of the “LIBio” by the "Impact Biomolecules" project of the "Lorraine Université d'Excellence" (Investissements d’avenir – ANR 15-004). The authors would like to thank the Laboratoire de chimie du solide minéral (Université de Lorraine, Nancy) for the SEM observations and the Laboratoire de Chimie Physique et de Microbiologie pour l’Environnement (Université de Lorraine, Nancy) for XPS analysis and AFM measurements (Rana OMAR).

References

Andre, C., Richard, B., Le Page, J.-F., Jeantet, R., Delaplace, G., 2012. Influence of Mixing System Design and Operating Parameters on Dissolution Process. Chem. Eng. Technol. 35, 247–254. https://doi.org/10.1002/ceat.201100441

Cogswell, S., Berger, S., Waterhouse, D., Bally, M.B., Wasan, E.K., 2006. A parenteral econazole formulation using a novel micelle-to-liposome transfer method: In Vitro characterization and tumor growth delay in a breast cancer xenograft model. Pharm. Res. 23, 2575–2585.

Eaton, P.J., West, P., 2010. Atomic force microscopy. Oxford University Press, Oxford ; New York.

459 Fabra, M.J., Márquez, E., Castro, D., Chiralt, A., 2011. Effect of maltodextrins in the water-
460 content–water activity–glass transition relationships of noni (Morinda citrifolia L.) pulp
461 powder. J. Food Eng. 103, 47–51. https://doi.org/10.1016/j.jfoodeng.2010.09.018
462 Fang, Y., Selomulya, C., Ainsworth, S., Palmer, M., Chen, X.D., 2011. On quantifying the
463 dissolution behaviour of milk protein concentrate. Food Hydrocoll. 25, 503–510.
464 https://doi.org/10.1016/j.foodhyd.2010.07.030
465 Fang, Z., Bhandari, B., 2011. Effect of spray drying and storage on the stability of bayberry
466 polyphenols. Food Chem. 129, 1139–1147.
467 https://doi.org/10.1016/j.foodchem.2011.05.093
468 Fitzpatrick, J.J., Ahrné, L., 2005. Food powder handling and processing: Industry problems,
469 knowledge barriers and research opportunities. Chem. Eng. Process. Process Intensif.
470 44, 209–214. https://doi.org/10.1016/j.cep.2004.03.014
471 Fitzpatrick, J.J., Weidendorfer, K., Teunou, E., 2000. Reconstitution of dairy powders to high
472 solids content in a stirred-tank: the effect of agitation. Milchwissenschaft 55, 437–440.
473 Forny, L., Marabi, A., Palzer, S., 2011. Wetting, disintegration and dissolution of agglomerated
474 water soluble powders. Powder Technol. 206, 72–78.
475 https://doi.org/10.1016/j.powtec.2010.07.022
476 Gabas, A.L., Telis, V.R.N., Sobral, P.J.A., Telis-Romero, J., 2007. Effect of maltodextrin and
477 arabic gum in water vapor sorption thermodynamic properties of vacuum dried
478 pineapple pulp powder. J. Food Eng. 82, 246–252.
479 https://doi.org/10.1016/j.jfoodeng.2007.02.029
480 Gaiani, C., 2006. Étude des mécanismes de réhydratation des poudres laitières : influence de
481 la structure et de la composition des poudres. INPL, Nancy.

Gaiani, C., Scher, J., Ehrhardt, J.J., Linder, M., Schuck, P., Desobry, S., Banon, S., 2007b. Relationships between Dairy Powder Surface Composition and Wetting Properties during Storage: Importance of Residual Lipids. J. Agric. Food Chem. 55, 6561–6567. https://doi.org/10.1021/jf070364b

Gaiani, C., Scher, J., Schuck, P., Desobry, S., Banon, S., 2009. Use of a turbidity sensor to determine dairy powder rehydration properties. Powder Technol. 190, 2–5. https://doi.org/10.1016/j.powtec.2008.04.042

Gaiani, C., Scher, J., Schuck, P., Hardy, J., Desobry, S., Banon, S., 2006. The dissolution behaviour of native phosphocaseinate as a function of concentration and temperature using a rheological approach. Int. Dairy J. 16, 1427–1434. https://doi.org/10.1016/j.idairyj.2005.12.004

Gaiani, C., Schuck, P., Scher, J., Desobry, S., Banon, S., 2007a. Dairy Powder Rehydration: Influence of Protein State, Incorporation Mode, and Agglomeration. J. Dairy Sci. 90, 570–581. https://doi.org/10.3168/jds.S0022-0302(07)71540-0

Goalard, C., Samimi, A., Galet, L., Dodds, J.A., Ghadiri, M., 2006. Characterization of the Dispersion Behavior of Powders in Liquids. Part. Part. Syst. Charact. 23, 154–158. https://doi.org/10.1002/ppsc.200601024

Goula, A.M., Adamopoulos, K.G., 2010. A new technique for spray drying orange juice concentrate. Innov. Food Sci. Emerg. Technol. 11, 342–351. https://doi.org/10.1016/j.ifset.2009.12.001

Hogekamp, S., Schubert, H., 2003. Rehydration of Food Powders. Food Sci. Technol. Int. 9, 223–235. https://doi.org/10.1177/1082013203034938

Islam, M.Z., Kitamura, Y., Yamano, Y., Kitamura, M., 2016. Effect of vacuum spray drying on the physicochemical properties, water sorption and glass transition phenomenon of

orange juice powder. J. Food Eng. 169, 131–140. https://doi.org/10.1016/j.jfoodeng.2015.08.024

Jadhav, N.R., Gaikwad, V.L., Nair, K.J., Kadam, H.M., 2009. Glass transition temperature: Basics and application in pharmaceutical sector. Asian J. Pharm. AJP Free Full Text Artic. Asian J Pharm 3.

Jeantet, R., Schuck, P., Six, T., Andre, C., Delaplace, G., 2010. The influence of stirring speed, temperature and solid concentration on the rehydration time of micellar casein powder. Dairy Sci. Technol. 90, 225–236. https://doi.org/10.1051/dst/2009043

Jiang, H., Zhang, M., Adhikari, B., 2013. Fruit and vegetable powders, in: Handbook of Food Powders. Elsevier, pp. 532–552. https://doi.org/10.1533/9780857098672.3.532

Kleinebudde, P., 2004. Roll compaction/dry granulation: pharmaceutical applications. Eur. J. Pharm. Biopharm. 58, 317–326. https://doi.org/10.1016/j.ejpb.2004.04.014

Liu, F., Cao, X., Wang, H., Liao, X., 2010. Changes of tomato powder qualities during storage. Powder Technol. 204, 159–166. https://doi.org/10.1016/j.powtec.2010.08.002

Lopez-Quiroga, E., Prosapio, V., Fryer, P.J., Norton, I.T., Bakalis, S., 2019. Model discrimination for drying and rehydration kinetics of freeze-dried tomatoes. J. Food Process Eng. https://doi.org/10.1111/jfpe.13192

Mitchell, W.R., Forny, L., Althaus, T., Niederreiter, G., Palzer, S., Hounslow, M.J., Salman, A.D., 2019. Surface tension-driven effects in the reconstitution of food powders. Chem. Eng. Res. Des. 146, 464–469. https://doi.org/10.1016/j.cherd.2019.04.015

Mitchell, W.R., Forny, L., Althaus, T.O., Niederreiter, G., Palzer, S., Hounslow, M.J., Salman, A.D., 2015. Mapping the rate-limiting regimes of food powder reconstitution in a standard mixing vessel. Powder Technol. 270, 520–527. https://doi.org/10.1016/j.powtec.2014.08.014

530 Moghbeli, S., Jafari, S.M., Maghsoudlou, Y., Dehnad, D., 2019. Influence of pectin-whey
531 protein complexes and surfactant on the yield and microstructural properties of date
532 powder produced by spray drying. J. Food Eng. 242, 124–132.
533 https://doi.org/10.1016/j.jfoodeng.2018.08.025
534 Murrieta-Pazos, I., Gaiani, C., Galet, L., Scher, J., 2012. Composition gradient from surface to
535 core in dairy powders: Agglomeration effect. Food Hydrocoll. 26, 149–158.
536 https://doi.org/10.1016/j.foodhyd.2011.05.003
537 Nijdam, J.J., Langrish, T.A.G., 2006. The effect of surface composition on the functional
538 properties of milk powders. J. Food Eng. 77, 919–925.
539 https://doi.org/10.1016/j.jfoodeng.2005.08.020
540 Rajniak, P., Mancinelli, C., Chern, R., Stepanek, F., Farber, L., Hill, B., 2007. Experimental study
541 of wet granulation in fluidized bed: Impact of the binder properties on the granule
542 morphology. Int. J. Pharm. 334, 92–102.
543 https://doi.org/10.1016/j.ijpharm.2006.10.040
544 Richard, B., Le Page, J.F., Schuck, P., Andre, C., Jeantet, R., Delaplace, G., 2013. Towards a
545 better control of dairy powder rehydration processes. Int. Dairy J. 31, 18–28.
546 https://doi.org/10.1016/j.idairyj.2012.07.007
547 Roos, Y.H., 2002. Importance of glass transition and water activity to spray drying and stability
548 of dairy powders. Le Lait 82, 475–484. https://doi.org/10.1051/lait:2002025
549 Rouxhet, P.G., Misselyn-Bauduin, A.M., Ahimou, F., Genet, M.J., Adriaensen, Y., Desille, T.,
550 Bodson, P., Deroanne, C., 2008. XPS analysis of food products: toward chemical
551 functions and molecular compounds. Surf. Interface Anal. 40, 718–724.
552 https://doi.org/10.1002/sia.2779
553 Schubert, H., 1993. Instantization of powdered food products. Int. Chem. Eng. 33, 28–45.

554 Tonon, R.V., Baroni, A.F., Brabet, C., Gibert, O., Pallet, D., Hubinger, M.D., 2009. Water
555 sorption and glass transition temperature of spray dried açai (Euterpe oleracea Mart.)
556 juice. J. Food Eng. 94, 215–221. https://doi.org/10.1016/j.jfoodeng.2009.03.009
557 Wangler, J., Kohlus, R., 2018. Development and validation of methods to characterize
558 rehydration behavior of food hydrocolloids. Food Hydrocoll. 82, 500–509.
559 https://doi.org/10.1016/j.foodhyd.2018.04.018
560 Wangler, J., Teichmann, H., Konstanz, E., Kohlus, R., 2019. Experimental investigation and
561 simulation of rehydration dynamics of biopolymer powders. Powder Technol. 355,
562 461–473. https://doi.org/10.1016/j.powtec.2019.07.022
563

Figures and Captions.

Figure 1. Macroscopic and microscopic views of the fruit powders studied. Top: powders before compaction process (FNC, RNC and PNC). Bottom: powders after compaction process (FC, RC and PC).

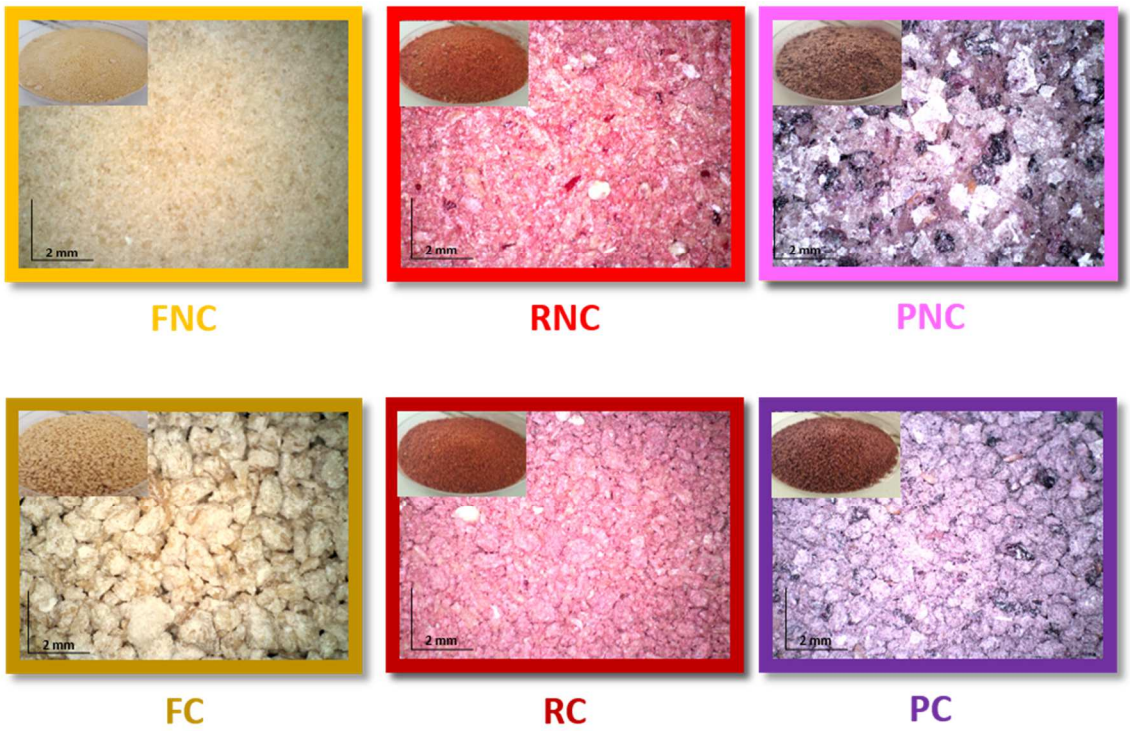

Figure 2. Particle size distribution functions of the six fruit powders studied at the two water activity values ($a_w \sim 0$ and ~ 0.35).

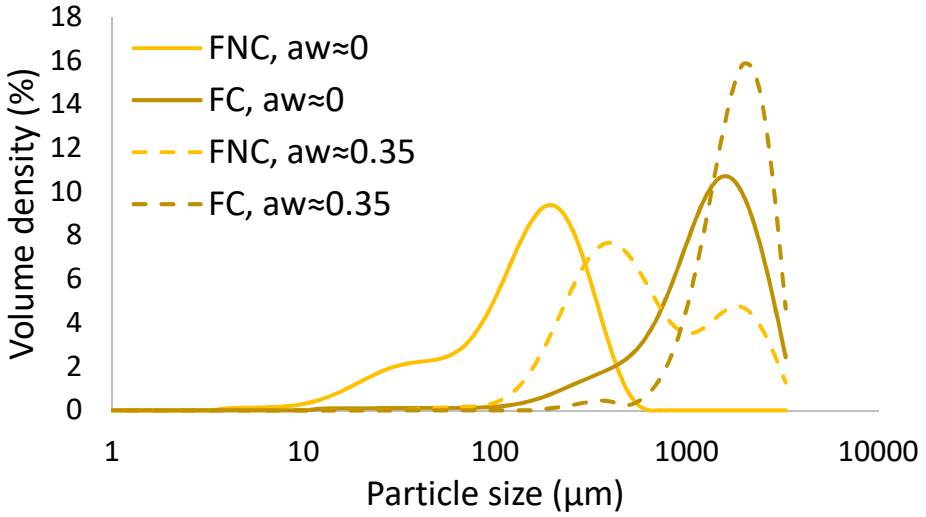

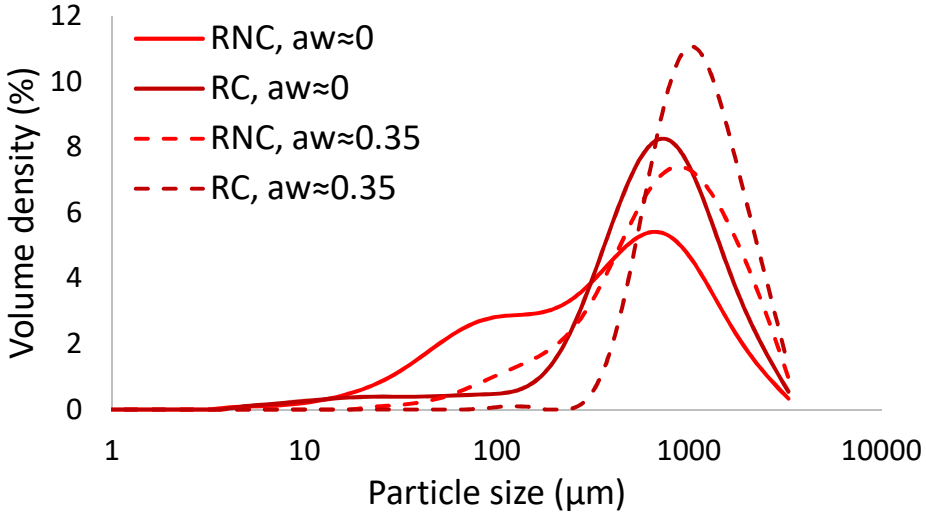

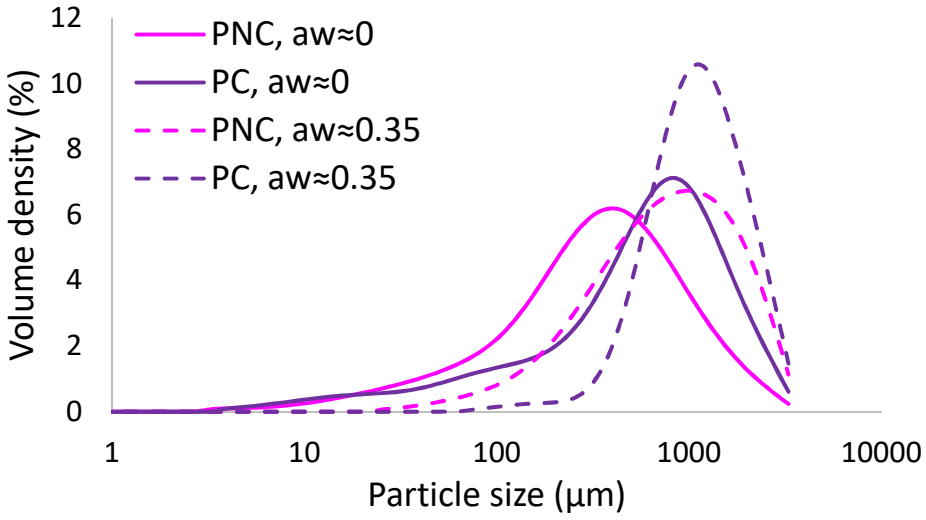

Figure 3. Pictures and microscopic images at two water activity values ($a_w \sim 0$ and ~ 0.35) of the six fruit powders studied (FNC, FC, RNC, RC, PNC and PC).

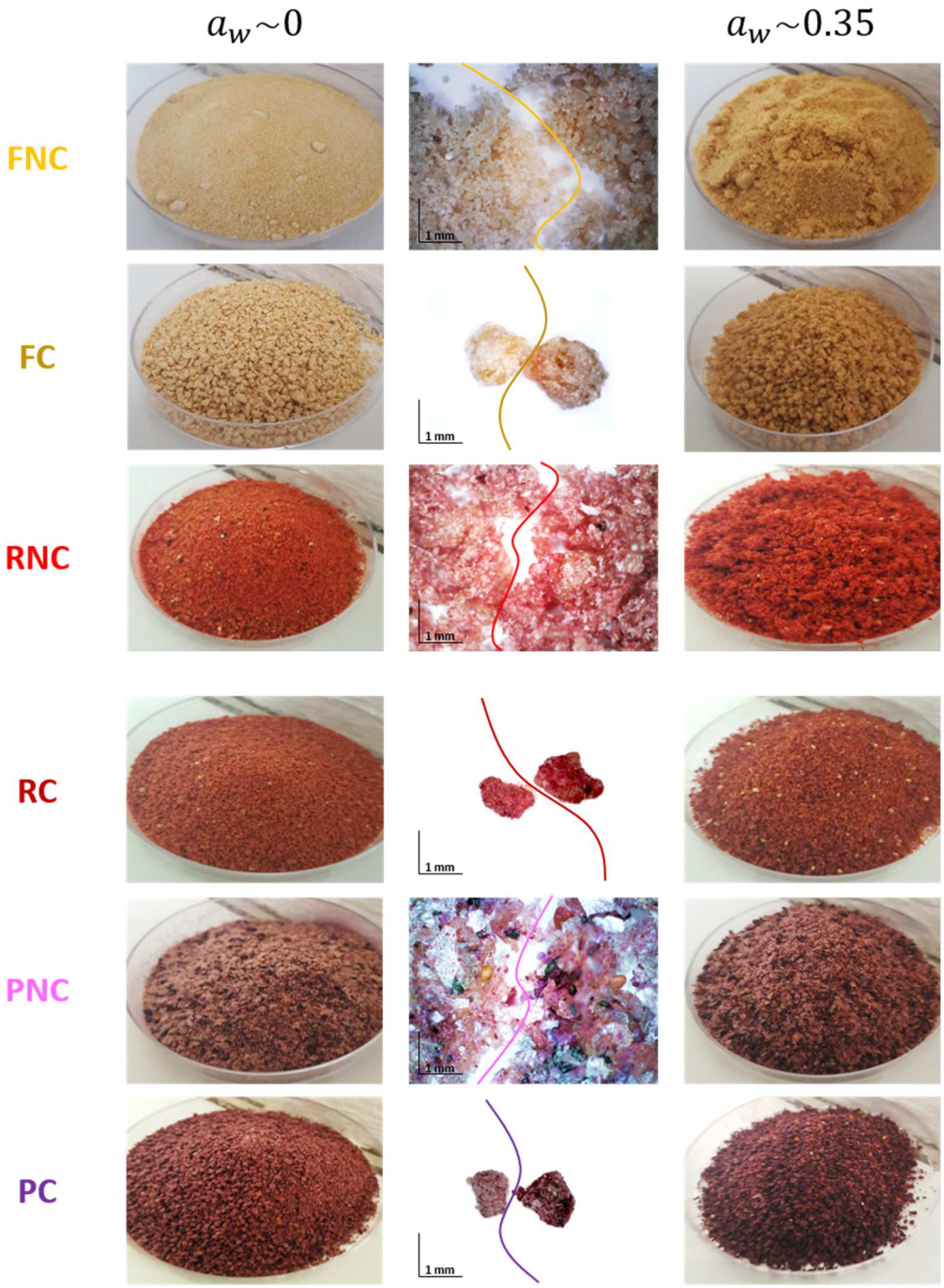

Figure 4. SEM images at various magnifications for the six fruit powders studied at both $a_w \sim 0$ and $a_w \sim 0.35$.

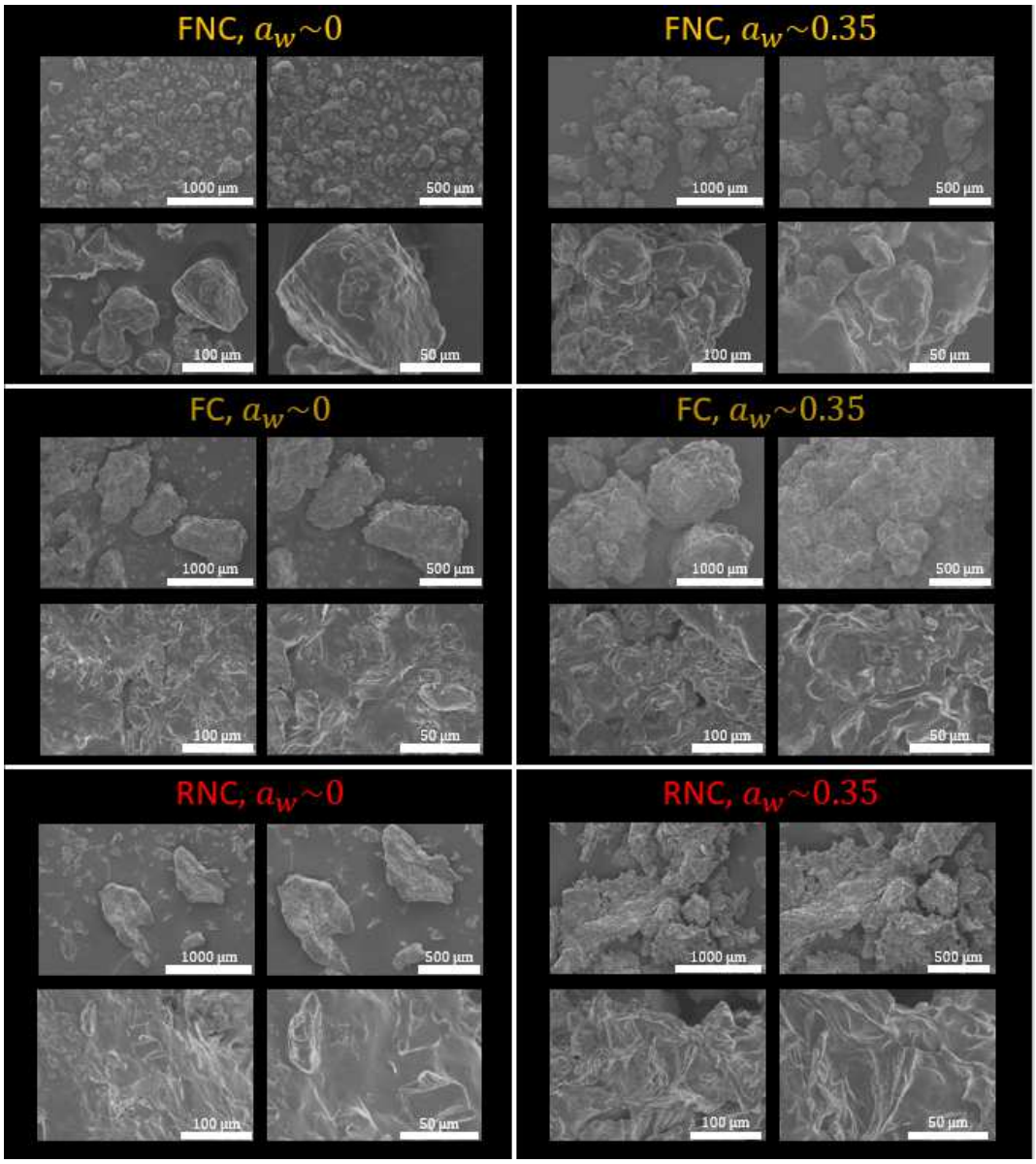

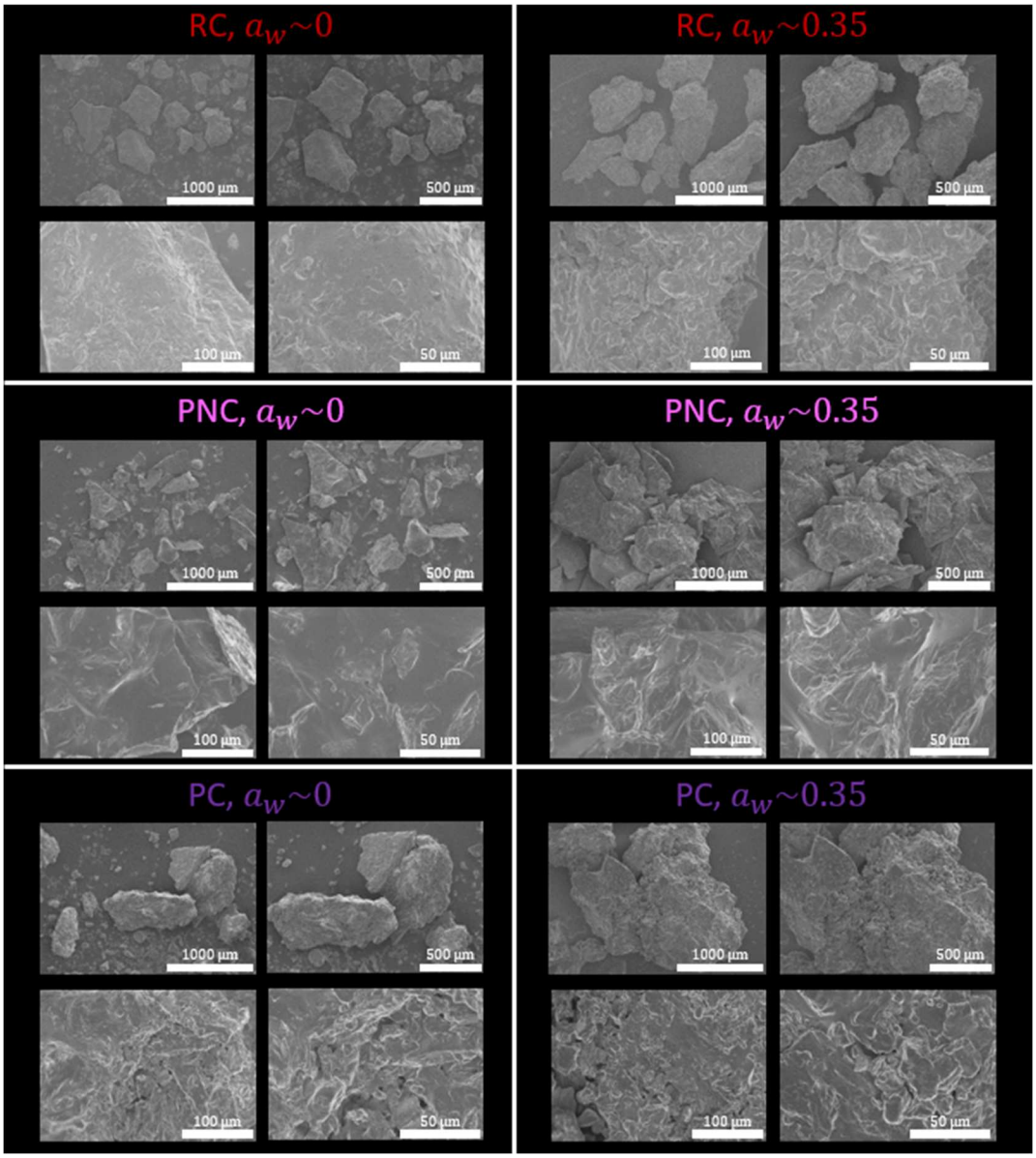
RC, a_w~0
1000 µm
500 µm
100 µm
50 µm
RC, a_w~0.35
1000 µm
500 µm
100 µm
50 µm
PNC, a_w~0
1000 µm
500 µm
100 µm
50 µm
PNC, a_w~0.35
1000 µm
500 µm
100 µm
50 µm
PC, a_w~0
1000 µm
500 µm
100 µm
50 µm
PC, a_w~0.35
1000 µm
500 µm
100 µm
50 µm

Figure 5. (a) Surface atomic concentration of chemical elements, (b) proportion of carbon bonds and (c) proportion of carbon bonds ratios detected at the surface of FNC and FC powders.

Elements	FNC	FC
$\mathbf{C_{1s}}$	70.92 ± 0.13	73.38 ± 1.96
$\mathbf{O_{1s}}$	27.05 ± 0.18	25.39 ± 1.91
$\mathbf{N_{1s}}$	1.79 ± 0.10	1.23 ± 0.12
$\mathbf{K_{2p}}$	0.15 ± 0.03	--
$\mathbf{P_{2p}}$	0.09 ± 0.09	--

(a)

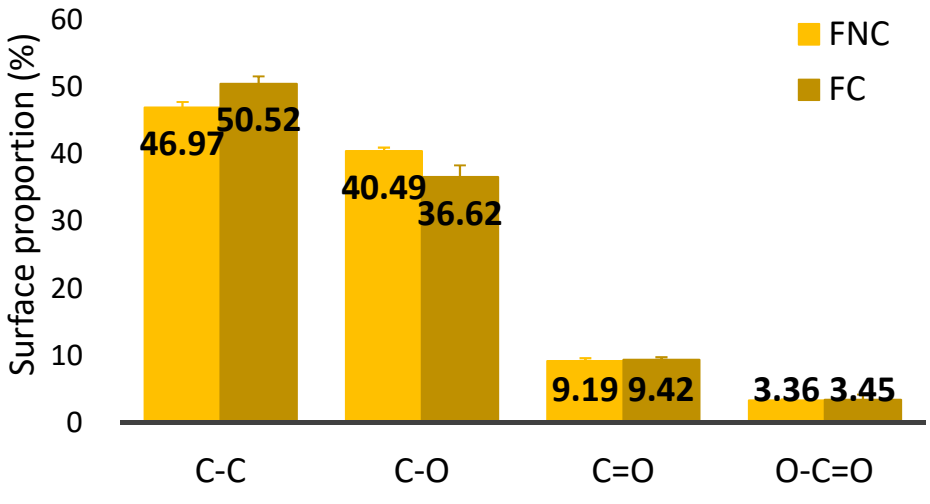

(b)

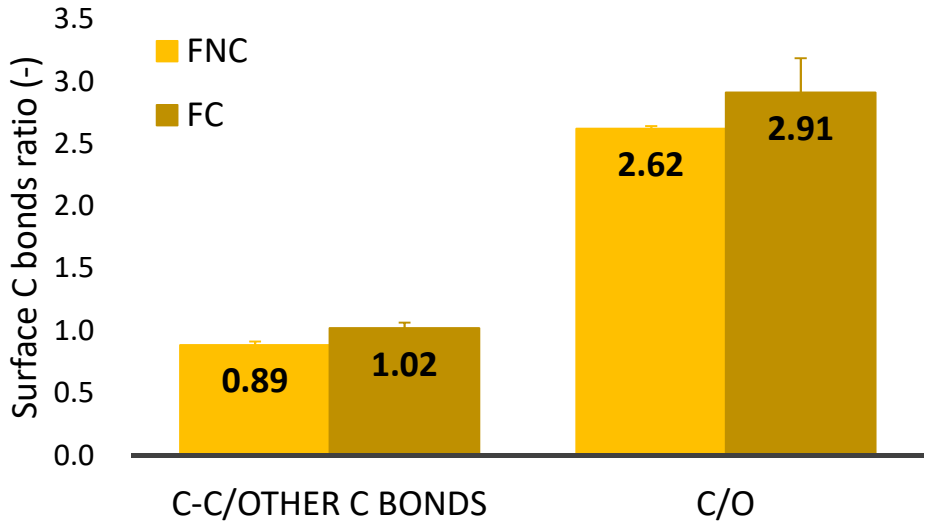

(c)

Figure 6. Surface topography at two water activity values for RC powder and corresponding distribution of the elastic modulus after curve fitting with the Sneddon model. Inserts in histograms represent the associated elasticity maps.

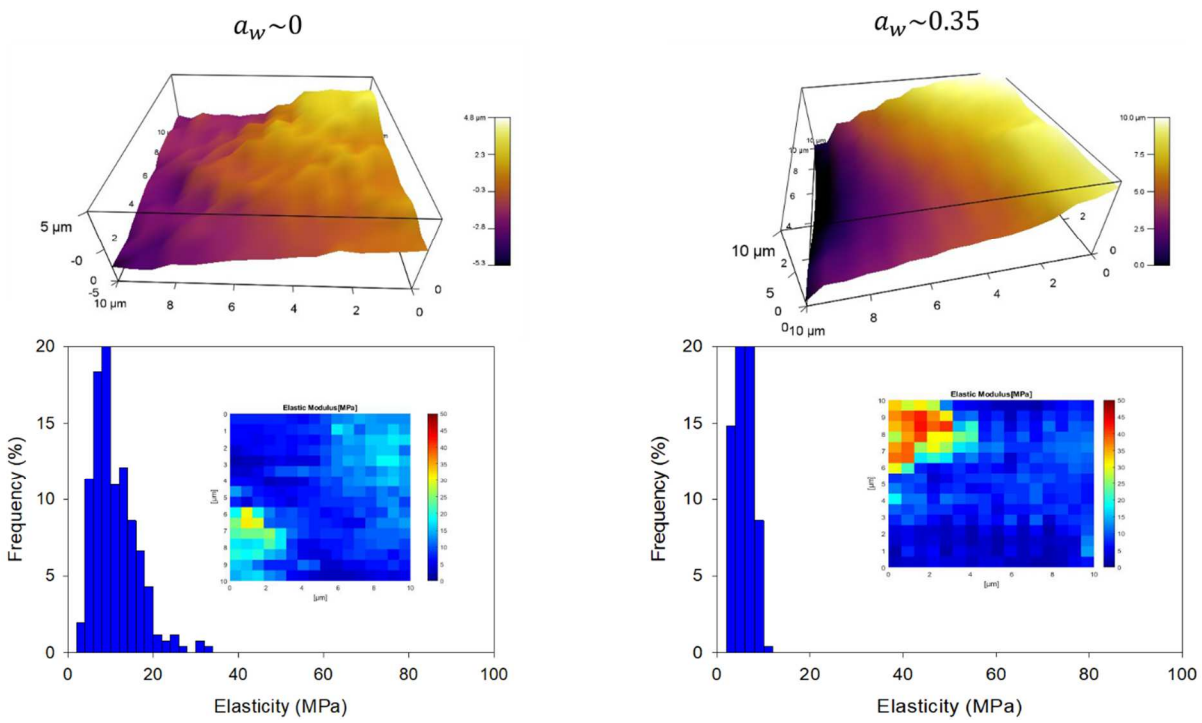

Figure 7. Evolution of the rehydration time as a function of the stirring speed value N at a fixed water temperature T=25 °C, and at different water activity values for (a) FNC and FC powders, (b) RNC and RC powders and (c) PNC and PC powders.

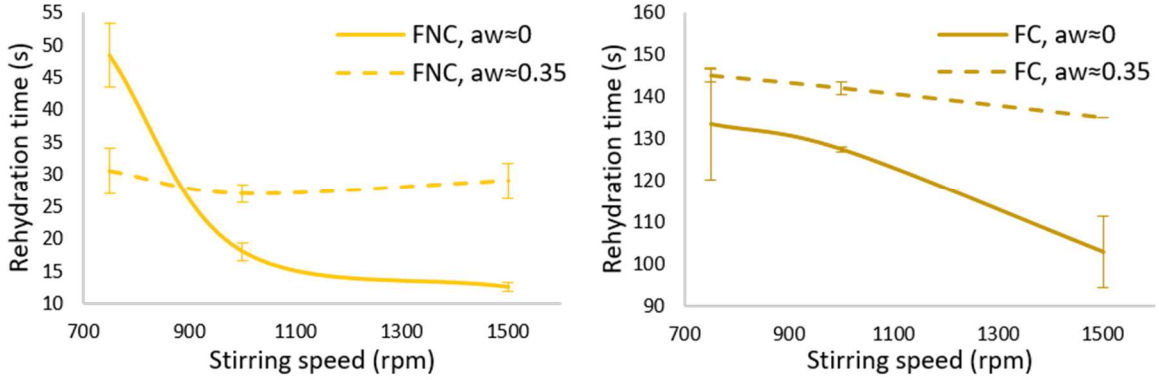

(a)

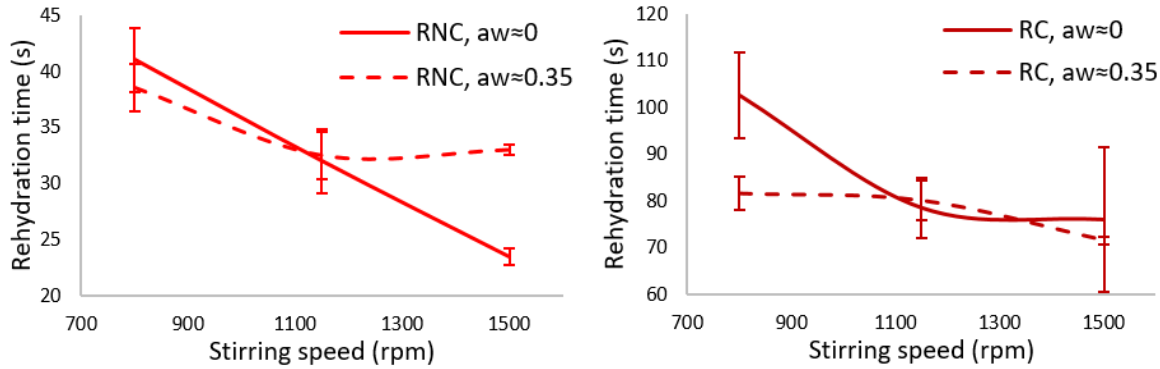

(b)

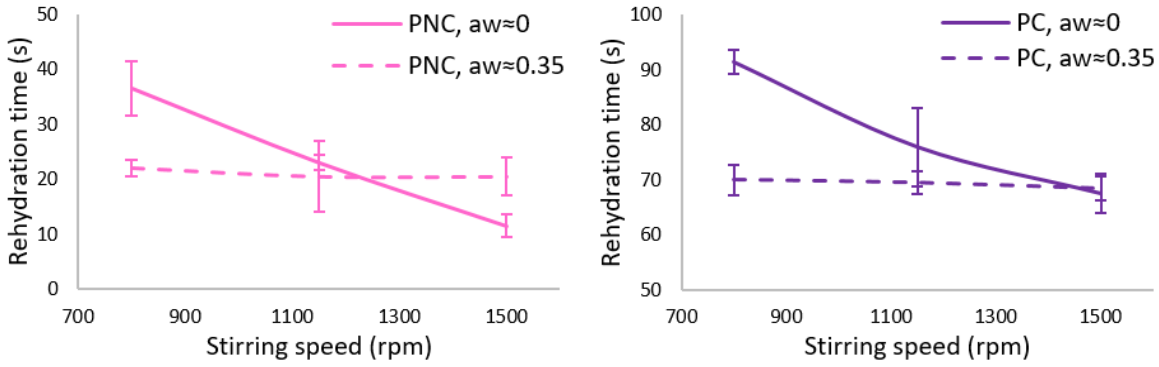

(c)

Figure 8. At both $a_w \sim 0$ and $a_w \sim 0.35$, for (a) FNC powder and (b) FC powder. Left: Maps presenting the time evolution of the volume density function. Right: Volume density function at $t_{initial}$ (dry powder) and t_{final} (powder entirely rehydrated).

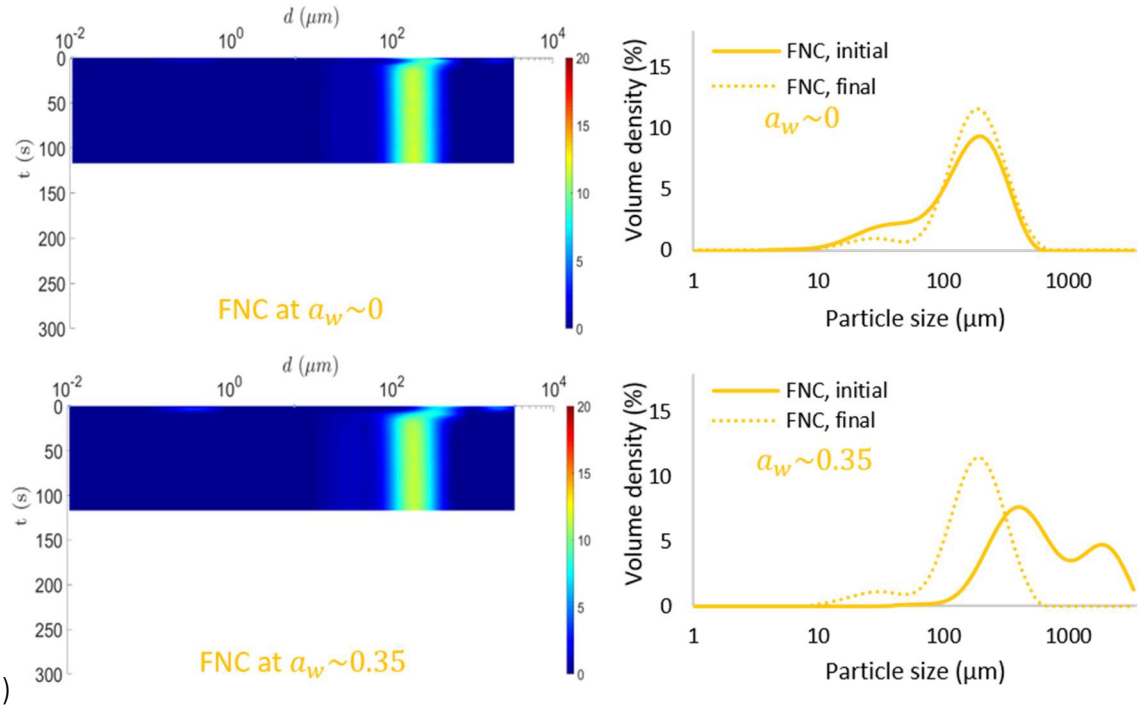

(a)

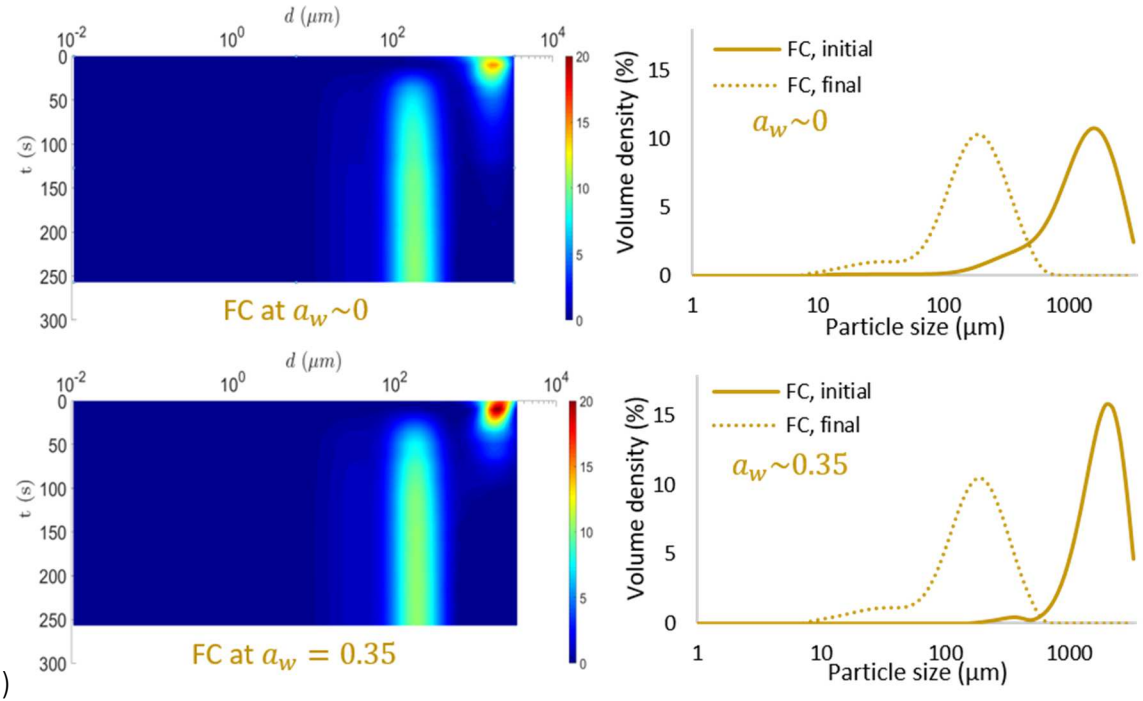

(b)

Figure 9. Logarithmic plot of the time evolution of the mean diameter d_{50} extracted from volume density functions for FNC and FC powders, at $a_w \sim 0$ and $a_w \sim 0.35$. The data are well fitted to equation 2 (solid lines and dotted lines).

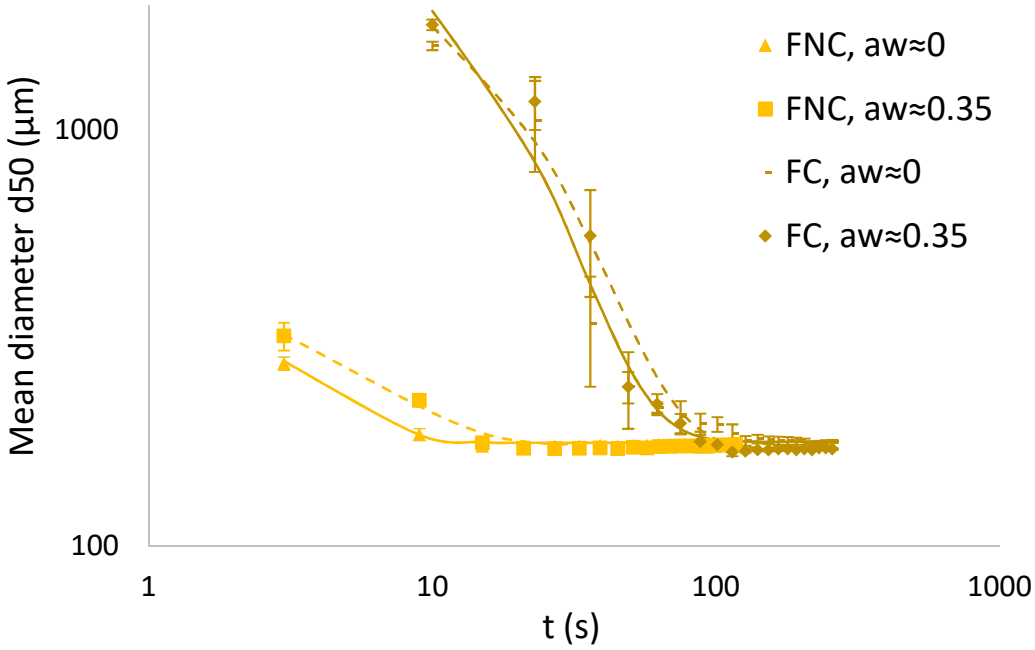

Figure 10. Summary of the relevant results in term of physicochemical properties from macro- to nano- scale for fruit powders.

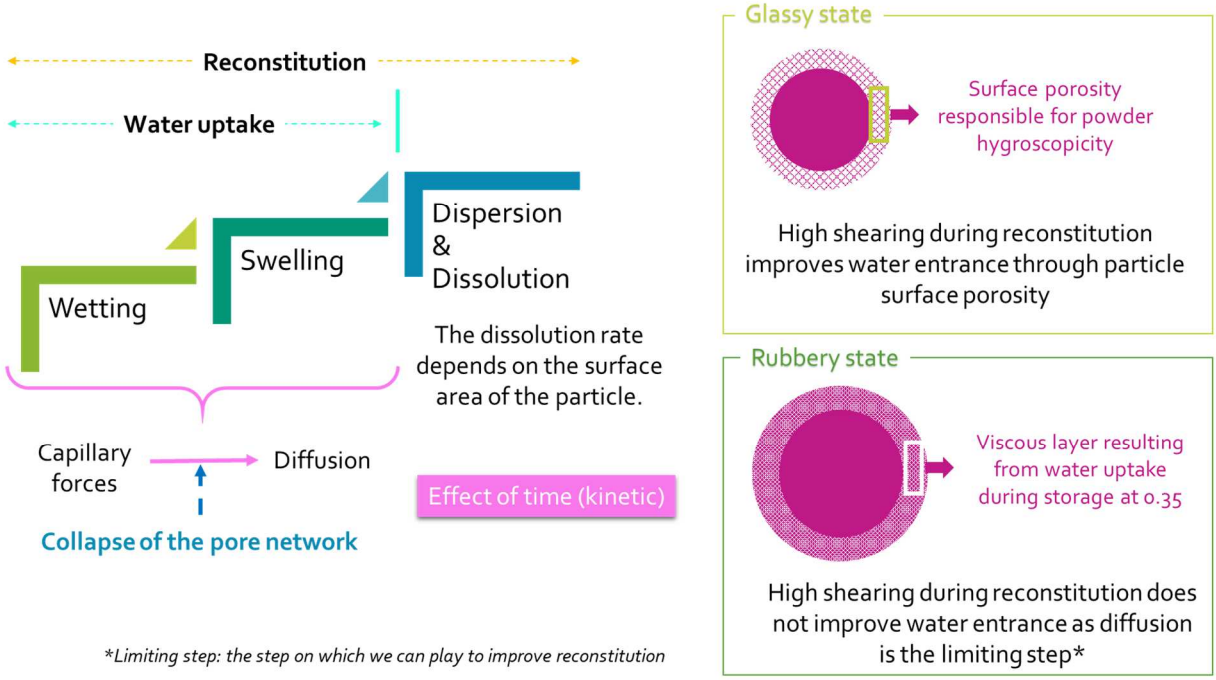

Table of content

Table 1. Information related to particle size distribution functions of the six fruit powders studied at $a_w \sim 0$ and $a_w \sim 0.35$.

		d_{50} (μm)	span	% increase d_{50} with water activity
FNC	$a_w \sim 0$	152 ± 1	1.83 ± 0.04	270 %
	$a_w \sim 0.35$	563 ± 136	3.22 ± 1.34	
FC	$a_w \sim 0$	1330 ± 39	1.55 ± 0.10	10 %
	$a_w \sim 0.35$	1460 ± 148	1.26 ± 0.30	
RNC	$a_w \sim 0$	387 ± 46	3.36 ± 0.77	98 %
	$a_w \sim 0.35$	765 ± 3	2.30 ± 0.09	
RC	$a_w \sim 0$	671 ± 33	2.17 ± 0.24	59 %
	$a_w \sim 0.35$	1070 ± 53	1.49 ± 0.18	
PNC	$a_w \sim 0$	348 ± 17	3.12 ± 0.41	121 %
	$a_w \sim 0.35$	770 ± 18	2.38 ± 0.07	
PC	$a_w \sim 0$	634 ± 31	2.55 ± 0.18	74 %
	$a_w \sim 0.35$	1100 ± 69	1.54 ± 0.21	

Table 2. Endpoint glass transition temperatures T_g (°C) of the six fruit powders studied during the second heat rate, at $a_w \sim 0$ and $a_w \sim 0.35$.

	FNC	FC	RNC	RC	PNC	PC
$a_w \sim 0$	14.55 ± 0.18	24.92 ± 0.44	13.91 ± 0.14	17.71 ± 0.54	26.53 ± 1.98	24.73 ± 1.67
$a_w \sim 0.35$	-1.77 ± 1.64	-0.52 ± 1.02	-4.96 ± 1.85	-2.80 ± 1.02	1.91 ± 1.00	-4.28 ± 1.16

Table 3. Parameters values extracted from exponential time decay functions (Equation 2) for FNC and FC at $a_w \sim 0$ and $a_w \sim 0.35$: characteristic PSD rehydration time τ_{PSD} and final mean diameter value d_∞.

		τ_{PSD} (s)	d_∞ (µm)
FNC	$a_w \sim 0$	2.35 ± 0.09	177 ± 7
	$a_w \sim 0.35$	4.76 ± 0.21	175 ± 8
FC	$a_w \sim 0$	13.27 ± 0.01	178 ± 1
	$a_w \sim 0.35$	17.57 ± 0.45	171 ± 5